LBNL Report 56326

High efficiency, radiation-hard solar cells

Final report for the Director's Innovation Initiative project DII-2004-593 funded by the National Reconnaissance Office

October 22, 2004

Prepared by

J. W. Ager, Staff Scientist
Electronics Materials Program
Materials Sciences Division
Lawrence Berkeley National Laboratory

W. Walukiewicz, Senior Staff Scientist
Electronics Materials Program
Materials Sciences Division
Lawrence Berkeley National Laboratory

This work was supported by the Director's Innovation Initiative Program, National Reconnaissance Office, through the U.S. Department of Energy under Contract No. DE-AC03-76SF00098

Materials Sciences Division

Acknowledgements

We are grateful to a number of people at the Air Force Research Laboratory, Kirtland Air Force Base. We thank W. Kemp of the for performing the electron irradiation and D. Senft and H. Yoo for helpful discussions. We thank the group of A. Cartwright (U. Buffalo) for providing transient absorption and reflectivity measurements.

LBNL staff on the project included J. Wu, K. M. Yu, W. Shan, S. Li, and R. Jones. We thank Z. Liliental-Weber for providing TEM characterization that was supported by a separate AFOSR project.

Cornell (subcontractor) staff on the project included W. Schaff and H. Lu.

Acknowledgements 2
1 Executive Summary 4
2 Project Background 5
3 Project Technical Plan 7
4 Project Accomplishments 8
4.1 Task 1: High quality InGaN film growth 8
4.2 Task 2: Irradiation 10
4.3 Task 3: Evaluation of as-grown and irradiated films 11
4.4 Task 4: Radiation damage modeling 13
4.5 Task 5: Predict radiation service limits 15
5 Technological Outlook 16
6 References 17

1 Executive Summary

The direct gap of the $In_{1-x}Ga_xN$ alloy system extends continuously from InN (0.7 eV, in the near IR) to GaN (3.4 eV, in the mid-ultraviolet). This opens the intriguing possibility of using this single ternary alloy system in single or multi-junction (MJ) solar cells of the type used for space-based surveillance satellites. To evaluate the suitability of $In_{1-x}Ga_xN$ as a material for space applications, high quality thin films were grown with molecular beam epitaxy and extensive damage testing with electron, proton, and alpha particle radiation was performed. Using the room temperature photoluminescence intensity as a indirect measure of minority carrier lifetime, it is shown that $In_{1-x}Ga_xN$ retains its optoelectronic properties at radiation damage doses at least 2 orders of magnitude higher than the damage thresholds of the materials (GaAs and GaInP) currently used in high efficiency MJ cells. This indicates that the $In_{1-x}Ga_xN$ is well-suited for the future development of ultra radiation-hard optoelectronics. Critical issues affecting development of solar cells using this material system were addressed. The presence of an electron-rich surface layer in InN and $In_{1-x}Ga_xN$ ($0 < x < 0.63$) was investigated; it was shown that this is a less significant effect at large *x*. Evidence of p-type activity below the surface in Mg-doped InN was obtained; this is a significant step toward achieving photovoltaic action and, ultimately, a solar cell using this material.

2 Project Background

As shown in Fig. 1, the fundamental direct band gap range of the III-nitride alloy system is the widest of any compound semiconductor, extending from InN (0.7 eV, near-IR), to GaN (3.4, mid-UV), and finally to AlN (6.2 eV, deep-UV) [Wu *et al.*, 2002; Pereira *et al.*, 2001; Shan *et al.*, 1998; Kim *et al.*, 1997; Wu *et al.*, 2003a, Wu *et al.*, 2003b]. In the specific case of $In_{1-x}Ga_xN$, varying x between 0 and 0.63 produces direct bandgaps between 0.7 and 1.9 eV, which provides an excellent match to the useful part of the solar spectrum. In fact, current production and prototype high efficiency multijunction (MJ) solar cells use components with bandgaps in this range: Ge (0.66 eV), GaAs (1.43 eV), and GaInP (1.9 eV) [Bertness *et al.*, 1994; Yamaguchi *et al.*, 2003; Green *et al.*, 2003]. The highest efficiency MJ cells have up to 20 different layers, including the tunnel junctions, and require the use of a number of precursor streams in the deposition process (typically Al, In, Ga, As, and P). In this context, the possibility of designing and fabricating multi-junction solar cells using a single ternary alloy system, with the flexibility of choosing the number and the bandgaps of the constituent junctions to optimize the device performance, is potentially attractive.

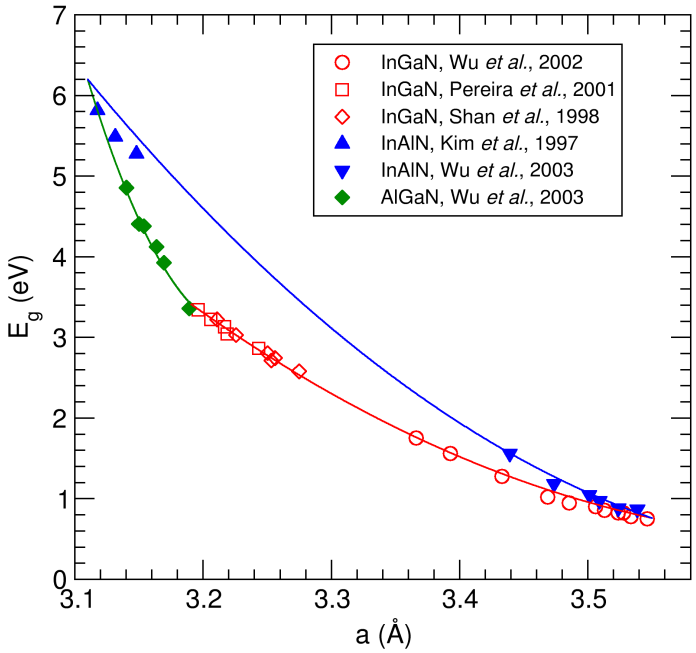

Fig. 1. Direct band gaps in InN-GaN-AlN ternary alloy system as a function of lattice constant *a*.

The fundamental properties of GaN, AlGaN, and Ga-rich InGaN have been rather thoroughly investigated [Vurgaftman and Meyer, 2003] and there are successful commercial products including green LEDs and lasers based on these materials. In contrast, growth of high-quality InN and In-rich InGaN epitaxial films has been achieved only relatively recently. Figure 2 demonstrates the improvement in electrical quality in molecular beam epitaxy (MBE) films grown in the Cornell III-V facility prior to the time period of this project. It is with this material that LBNL discovered in 2002 that the that the bandgap of InN is 0.7 eV [Wu *et al.*, 2002b]. Formerly it was believed to be 2.0 eV, in the red, and, for this reason, InN was not considered for solar cell applications.

Since space is the primary application of MJ solar cells, radiation resistance is crucial. In initial testing with 2 MeV protons, we obtained evidence that InN was much more radiation resistant than GaAs and GaInP, two components of current MJ cells [Wu *et al.*, 2003a]. In this DII project, a comprehensive series of measurements on electron, proton, and alpha particle irradiated InN and InGaN was used to demonstrate the

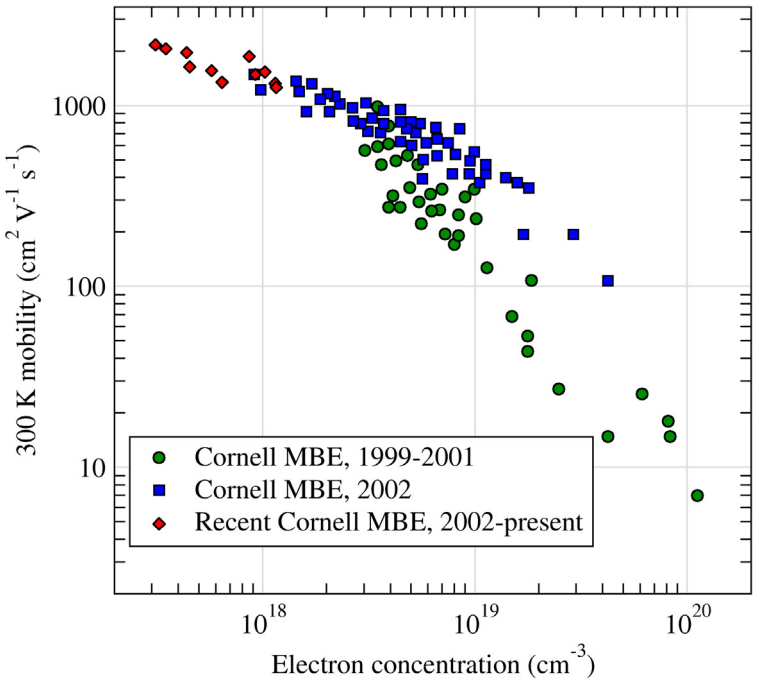

Fig. 2. Improvements in the growth of MBE films at the Cornell III-V laboratory have produced InN with electron concentrations $n < 4\text{x}10^{17}$ cm^{-3} and mobilities $\mu > 2000$ cm^2 V^{-1} s^{-1}.

extraordinary radiation hardness of this material. In addition, one of the main outstanding challenges in the photovoltaic applications of $In_{1-x}Ga_xN$ alloys, which include developing methods to achieve p-type doping and improving the structural quality of heteroepitaxial films, was also addressed.

3 Project Technical Plan

The project had 5 technical task which are summarized as follows.

1. Grow electronic quality films of InN and InGaN using molecular beam epitaxy (MBE) at the Cornell III-V growth laboratory (Cornell was a subcontractor to LBNL in the DII project). .
2. Expose InGaN films control materials used in current multijunction (MJ) solar cells (GaAs and GaInP) to high doses of high energy electrons and protons.
3. Evaluate the effects of radiation exposure on properties using standard optical and electronic techniques.
4. Model the radiation effects using the established damage displacement model; evaluate whether model is applicable at extremely high doses in the InN system.
5. Predict ultimate radiation service limits of InN and InGaN-based electronics.

4 Project Accomplishments

4.1 Task 1: High quality InGaN film growth

Growth of $In_{1-x}Ga_xN$ over the entire composition range has proven to be challenging due the presence of a significant miscibility gap at the growth temperatures required to maintain the stability of In-rich material [Ho and Stringfellow, 1996]. To our knowledge, all reported attempts to grow $In_{1-x}Ga_xN$ with $0.2 < x < 0.6$ and with a thickness useful for solar cells (*i.e.*, > 200 nm) by either MOCVD [Wakahara *et al.*, 1997; El-Masry *et al.*, 1998; Rao *et al.*, 2004] or MBE [Doppalapudi *et al.*, 1998] techniques resulted in phase separated material. We thus consider growth of uniform material in this composition range to be a significant achievement of the DII project.

InN and $In_{1-x}Ga_xN$ films were grown on sapphire substrates by molecular beam epitaxy [Lu *et al.*, 2000; Lu *et al.*, 2001]. Typically, an AlN nucleation layer and a GaN buffer layer were deposited prior to InN or InGaN growth. Film thicknesses ranged from 200 nm to over 7 μm. X-ray diffraction (XRD) using the AlN (0002) peak as the reference peak and Rutherford backscattering (RBS) were used to measure *x* in alloy films; the results of these two techniques were generally in excellent agreement. No evidence of In inclusions were observed in the XRD patterns in the films used in this study. As grown InN or In-rich InGaN films are always n-type with carrier concentrations as measured by Hall effect from high 10^{17} cm^{-3} to mid-10^{18} cm^{-3}. The low electron concentration InN films had room temperature mobilities in excess of 1000 cm^2 V^{-1} s^{-1}. Mobility decreased with *x* in $In_{1-x}Ga_xN$ films; for example, an $In_{0.37}Ga_{0.63}N$ film had a mobility of 13 cm^2 V^{-1} s^{-1}. Attempts were made to make p-type InN using Mg as a p-type dopant.

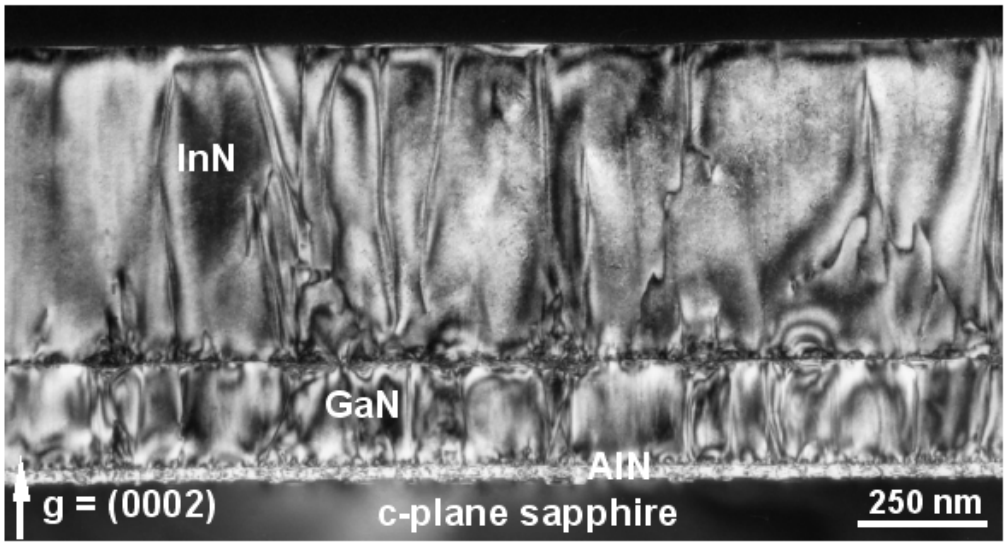

Fig. 3. This InN film has 5x10^{10} cm^{-2} dislocations: 80% edge, 5% screw, 15% mixed. Data courtesy of Z. Liliental-Weber, LBNL.

Transmission electron microscopy (TEM) was used to evaluate film quality. The high structural quality of InN films grown on GaN buffer layers is confirmed by the transmission electron micrograph shown in Fig. 3. For all of the optimized MBE-grown $In_{1-x}Ga_xN$ films studied the measured dislocation densities do not exceed mid-$10^{10}$$cm^{-2}$.

As a comparison, GaN films grown on sapphire by MBE typically have 10^9 dislocations cm^{-2}. Most of the dislocations were of edge character. Selected area electron diffraction (SAED) patterns consist of a single wurtzite InN diffraction pattern with no additional spots which could suggest the existence of secondary phases. Alloys were also of high

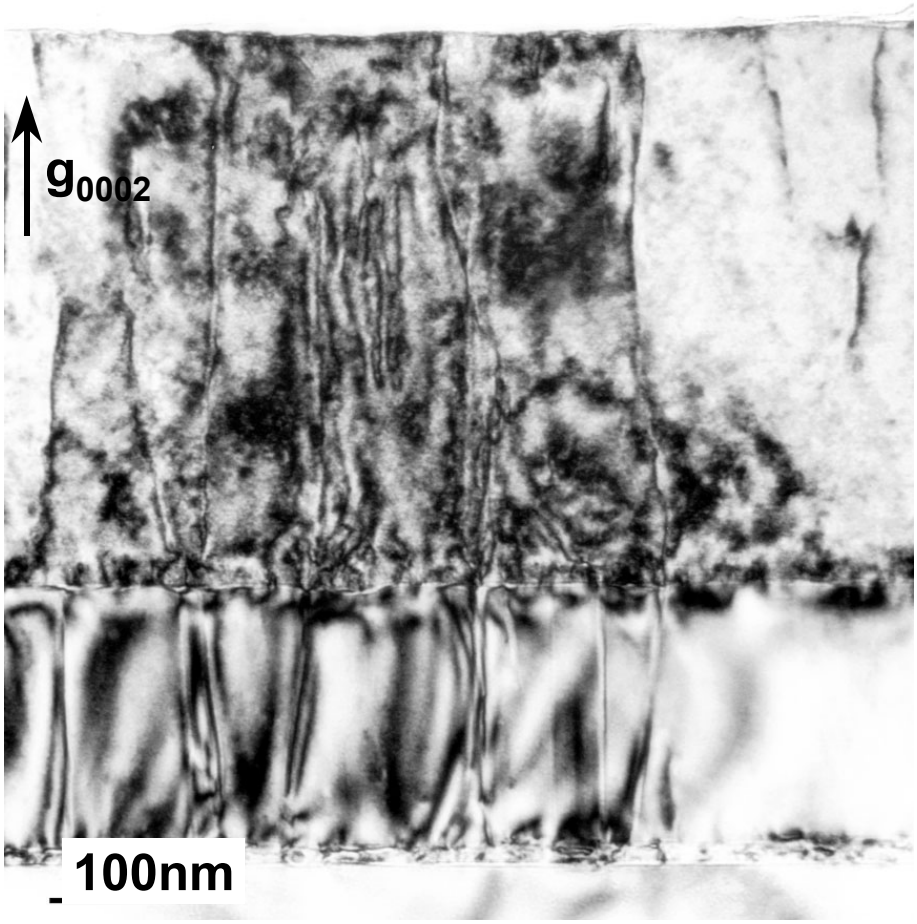

Fig. 4. TEM of sample GS1962 $In_{0.37}Ga_{0.63}N$, grown on a GaN buffer layer. This film is 400 nm thick and has a band gap of 1.9 eV. No evidence of phase separation is observed. Data courtesy of Z. Liliental-Weber, LBNL.

structural quality as shown in Fig. 4. In this case it is interesting to observe that some dislocations observed in the underlying GaN layer do not appear to propagate into the InGaN layer.

We found that non-optimized growth conditions could produce films which showed evidence of possible phase separation. Figure 5 compares the absorption and photoluminescence (PL) spectra of two films with similar composition grown on different buffer layers: GS 1513 $In_{0.5}Ga_{0.50}N$ grown on AlN and GS1962 $In_{0.47}Ga_{0.63}N$ grown on GaN. It is seen that there is a large "Stokes shift" between the absorption edge and the PL line in the film grown on AlN; this could be due to the presence of InGaN regions with higher In content than the average composition. The film grown on the GaN buffer has no observable Stokes shift and is compositionally uniform (see also Fig. 4). During the project, we demonstrated the ability to grow $In_{1-x}Ga_xN$ films up to $x = 0.6$ which had no Stokes shift and thus are likely to be compositionally uniform.

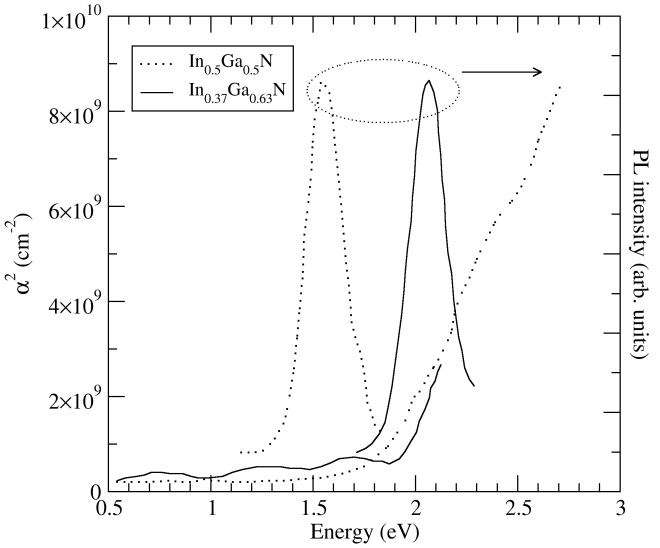

Fig. 5. Absorption (left hand axis) and PL (right hand axis) for InGaN films with bandgaps of 1.7 (dotted lines) and 1.9 eV (solid lines). The PL from the $In_{0.37}Ga_{0.63}N$ film occurs at the same energy as the fundamental band gap absorption; this film does not have a large "Stokes shift."

4.2 Task 2: Irradiation

High quality films with no "Stokes shift" were selected for the radiation study as summarized in the table.

Film	Composition	E_g (eV) (absorption)	E_g (PL)	n (cm^{-3}), μ ($cm^2 V^{-1} s^{-1}$)
GS1690	InN	0.63	0.67	$1x10^{18}$ 1560
GS1651	$In_{0.85}Ga_{0.15}N$	0.82	0.80	$1.43x10^{18}$ 700
GS1942	$In_{0.7}Ga_{0.3}N$	1.13	1.10	$2.3x10^{18}$ 40
GS1962	$In_{0.37}Ga_{0.63}N$	1.89	1.86	$1.1x10^{18}$ 20

High energy particle irradiation sources used were as follows.

Source	Description
LBNL van de Graaf accelerator	2 MeV protons up to $2x10^{15}$ cm^{-2} 2 MeV He^+ up to $2x10^{15}$ cm^{-2}
LBNL ion implanter	200 keV Ne^+
Kirtland AFB Dynamitron	1 MeV electrons up to $1x10^{17}$ cm^{-2}

All radiation was penetrating with respect to the InN or InGaN film (that is, the end of range was in the sapphire substrate). Particle doses were converted to non-ionizing energy loss (NIEL) using the methodology developed by the Naval Research Laboratory by using either standard tables for proton [Messenger *et al.*, 2000] and electron irradiation or the SRIM program for the case of alpha particles [Messenger *et al.*, 2002].

The NIEL was then used to calculate the corresponding displacement damage dose (D_d, units of MeV/g).

4.3 Task 3: Evaluation of as-grown and irradiated films

Methods used for evaluation of irradiated material are summarized as follows.

Method	Material property evaluated
Hall effect	Room temperature electron (majority carrier) concentration and mobility
Electrochemical capacitance-voltage (ECV) profiling	Carrier concentration and type vs. depth. Probe depth was about 10-15 nm.
Photoluminescence (PL) intensity	Band edge radiative recombination is limited by the minority carrier (hole) lifetime. Thus this technique is an indirect measurement of the minority carrier diffusion length.

During the time period of the project we were not able to fabricate a pn junction in InN or In-rich InGaN. This precluded direct testing of the effect of irradiation on power conversion efficiency in a prototype cell. We instead concentrated on evaluating the minority carrier (hole) lifetime. Extensive testing of standard MJ solar cells has established that the primary effect of radiation damage is to reduce the minority carrier diffusion length L, which then causes a drop in cell power [see Flood, 1998 and references therein]. Our approach was to use room temperature PL intensity as in indirect probe of L and hence as a predictor of solar cell performance.

We supported the validity of the PL intensity technique by performing direct measurements of the minority carrier lifetime on a number of our proton-irradiated films in collaboration with the University of Buffalo. The technique used was time resolved pump-probe transmission. This technique monitors the relaxation of a non-equilibrium charge distribution. The technique is, in general, sensitive to the minority carrier dynamics, holes in this case. The data from a number of as-grown films is summarized in the following table. Additional time resolved pump-probe transmission measurements were made on proton irradiated films for which (see below) no change in the PL intensity was observed. As a control, time resolved PL was performed on GaInP and GaN with identical protons doses. In the case of GaInP, the lowest dose lowered the PL lifetime from 750 ps to below the time resolution of the system (10 ps). A similar result was obtained for GaN; the lifetime was reduced from 125 ps to <10 ps after the lowest proton dose. In the InGaN films studied, the minority carrier lifetime was essentially unaffected by proton doses 10x up to the mid 10^{13} MeV/g. As a comparison, this dose reduces the power of a MJ solar cell to <20% of its BOL efficiency. These results are direct evidence of the radiation hardness of In-rich InGaN and also serve to validate the PL intensity technique.

Film	hole lifetime (ps)
GS 1690 InN	1100
GS 1942 $In_{0.68}Ga_{0.32}N$	41
GS 1962 $In_{0.37}Ga_{0.63}N$	40

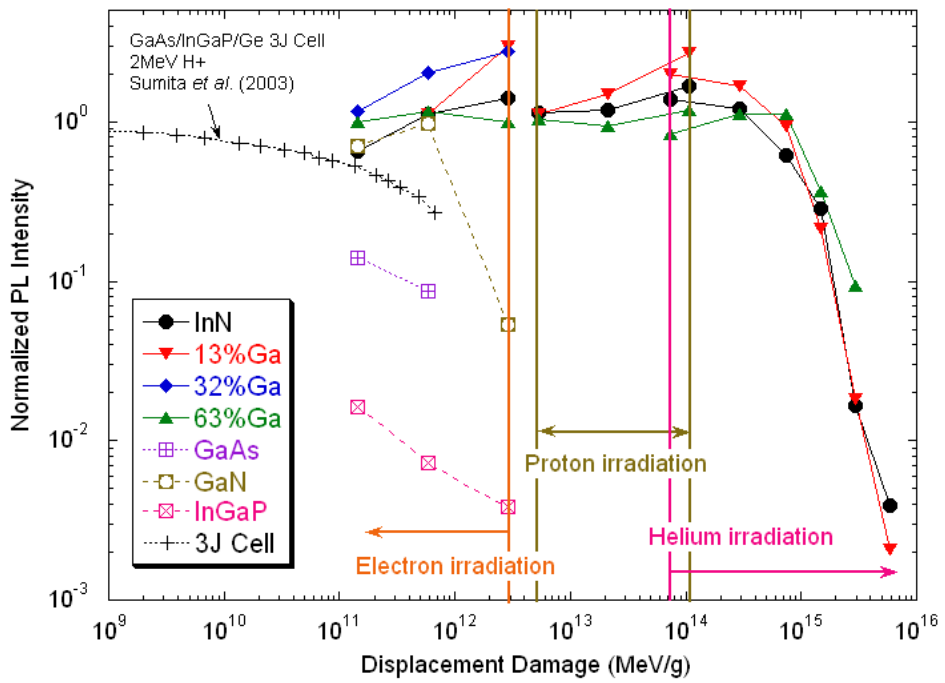

Fig. 6. Summary of the effect of 1 MeV electron, 2 MeV proton, and 2 MeV alpha particle irradiation on the relative room temperature PL intensity of InGaN alloys with bandgaps between 0.7 and 1.9 eV. PL data for GaAs and GaInP and literature data for solar cell power degradation as a function of D_d are also shown.

The room temperature PL intensity relative to unirradiated material as a function of radiation damage data is summarized in Fig. 6. Literature data for the power degradation of a typical high efficiency 3J GaInP/GaAs/Ge cell is shown for comparison [Sumita *et al.*, 2003]. PL data from GaAs and GaInP is also included in Fig. 6; however, the PL intensity became too weak to observe at the highest radiation doses in these materials. The data clearly confirm the radiation hardness of In-rich InGaN. For example, for a displacement damage dose D_d of 10^{12} MeV/g ($3x10^{16}$ cm^{-2} 1 MeV electrons), at which a typical MJ solar cell would be at 20% of its beginning of life (BOL) efficiency and the PL intensity of GaAs and GaInP degraded by at least a factor of ten, the InGaN films are unaffected. It is observed that a D_d near 10^{15} MeV/g is required to produce observable changes in the InGaN films.

An argument has been put forth that the radiation resistance of the In-rich InGaN alloys is due to the high density of structural defects in the as-grown material (that is, additional radiation damage has a smaller effect than it would in a material with an initial density of defects). To address this issue we have studied the effect of irradiation on the PL intensity of GaN films with a comparable density of structural defects as our InGaN films. As shown in Fig. 6 the PL intensity of GaN sample is much more sensitive to irradiation than that of In-rich GaInN films; effects are already observable at doses in the mid 10^{12} MeV/g range, which is 3 orders of magnitude less than the threshold for In-rich InGaN. This clearly demonstrates that the radiation resistance of In-rich InGaN is an intrinsic property of these materials.

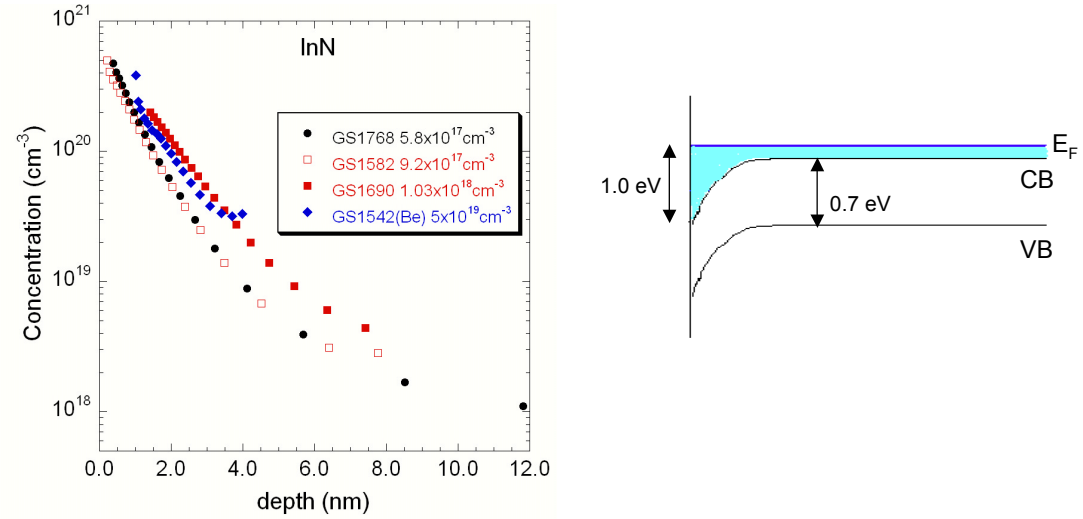

Fig. 7. (a) ECV profiles of InN films with different bulk electron concentrations. The surface electron carrier concentration is higher than in the bulk. (b) Diagram showing Fermi level pinning.

During the course of the project, the existence of a electron-rich surface accumulation layer in InN was reported [Mahboob *et al.*, 2004]. We investigated this in detail by using the electrochemical capacitance-voltage (ECV) technique to obtain carrier concentration profiles in InN films. The depletion profiles of a series of InN samples with different bulk electron concentration are shown in Fig. 7(a). A surface accumulation region in the range of 4-8 nm thick is observed for all of the samples. An electron concentration in the surface accumulation region as high as $5x10^{20}cm^{-3}$ is measured. We have also looked at the surface accumulation layer as a function of x in $In_{1-x}Ga_xN$. Figure 8 shows a series of depletion profiles for $In_{1-x}Ga_xN$ samples with x ranging from 0 to 0.63. Increasing Ga content in InGaN results in a reduction of the surface electron concentration by an order of magnitude over the range of x measured. This is consistent with our model of the Fermi stabilization energy in this alloy system, as discussed in Section 4.4 below.

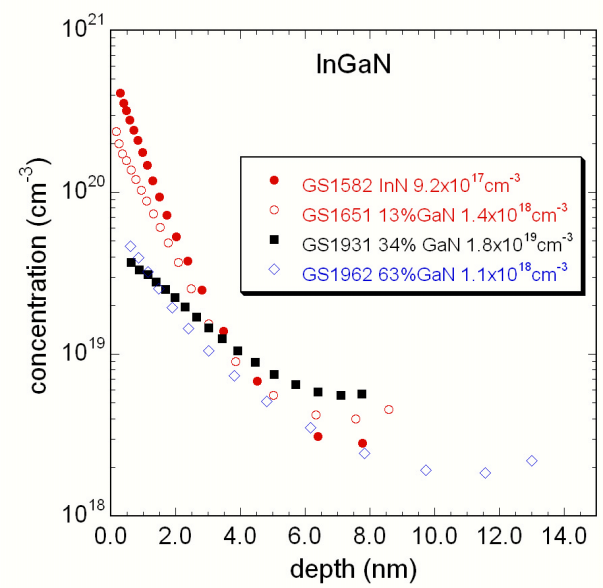

Fig. 8. ECV measurements of the electron concentration near the surface in In1-xGaxN films with $0 < x < 0.63$. The films have approximately the same bulk electron concentration in the low 10^{18} cm^{-3} range. Electron accumulation at the surface is observed in all cases. The effect is the strongest in InN and decreases with increasing x as E_{FS} (see Fig. 9) moves closer to the conduction band edge.

4.4 Task 4: Radiation damage modeling

A number of important technological and fundamental properties of semiconductors,

including the degree to which they can be doped n- and p-type and their response to the presence of native defects, can be understood within the amphoteric native defect model [Walukiewicz, 1989; Walukiewicz, 2001]. The model considers the energy locations of charge transition states associated with native defects (which include broken bonds and vacancies caused by irradiation). In most semiconductors, this occurs at a specific energy with respect to the vacuum level and thus forms a universal energy reference known as the Fermi stabilization level (E_{FS}).

Here we apply this model to understand the observed radiation hardness of In-rich InGaN, as well as some of the other properties observed experimentally. The location of

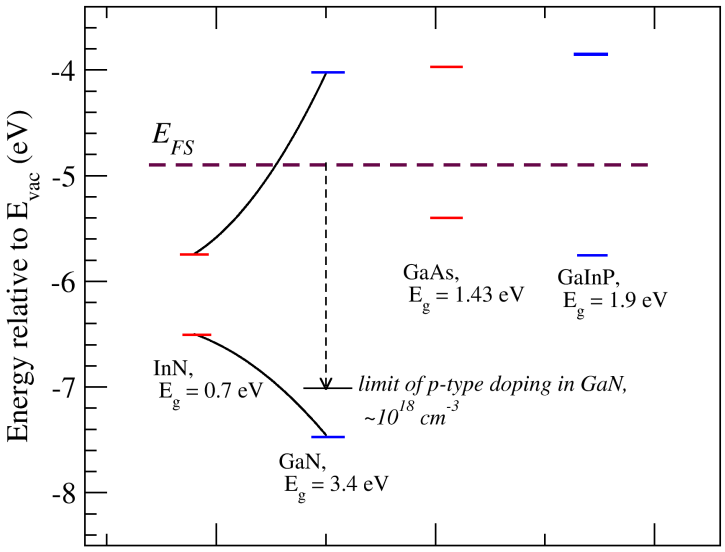

Fig. 9. Position of the Fermi stabilization energy E_{FS} with respect to the valence and conduction band edge energy (measured relative to the vacuum level for InN, GaN, GaAs, and GaInP). It is known that E_{FS} lies ~ 0.9 eV below the conduction band edge in GaN; the value for InN was then determined based on the known VB offset between GaN and InN. The degree to which E_F can be lowered in GaN by p-type doping with Mg is also indicated.

E_{FS} is depicted in Fig. 9 for InN, GaN, and two materials used in existing MJ cells, GaAs and GaInP. For GaAs and GaInP, E_{FS} is located within the bandgap. In the case of GaAs, it lies closer to the valence band edge (VBE). It has been recognized that defect levels located near the mid-gap position are the most effective non-radiative recombination centers. These defects provide fast non-radiative recombination centers in GaAs and GaInP, which reduce the minority carrier diffusion length in MJ solar cells, leading to degradation of performance. In this context, InN is an extreme case with E_{FS} is located deep in the conduction band. High energy barriers for the carrier recombination through the dangling-bond-like defect states prevents these defects from acting as efficient recombination centers; we would then predict that InN and In-rich InGaN should be relatively insensitive to radiation damage.

The model can also be applied to make predictions about doping and surface properties. For example, the model provides an explanation for the well-known p-type behavior of as-grown GaAs and the limitation of obtaining n-GaAs with high n; if the Fermi level E_F is pushed too high above E_{FS}, compensating native defects will form, lowering the effective electron concentration. Examination of the E_{FS} trends in Fig. 9

produces a prediction that in In-rich InGaN the surface dangling bond states with the energies well above the conduction band edge resulting in an accumulation of surface electrons in these materials. Moreover, the dangling-bond-like states on the surface of these materials should tend to pin the surface Fermi energy at E_{FS} irrespective of the doping condition in the bulk. This was indeed what was observed [Fig. 7(a)]. The high surface electron concentration is consistent with our experience that all metals form ohmic contacts to these materials. As x increases, E_{FS} moves closer to the CBE. Therefore, as expected, the surface electron concentration decreases with increasing Ga content from 4.3×10^{20} cm^{-3} in InN to $3.5 \times 10^{19} cm^{-3}$ in $In_{0.37}Ga_{0.63}N$ as EFS becomes closer to the CB edge (see Fig. 8).

Furthermore, the configuration of the CB edge and valence band (VB) edges of In-rich InGaN with respect to E_{FS} can be seen to be consistent with the asymmetry in the doping efficiency in these materials: they are n-type as grown, and p-type doping is intrinsically difficult. For InN, E_{FS} lies inside the conduction band; this explains the strong n-type behavior of as-grown material and will create challenges in obtaining p-type material. However, as illustrated in Fig. 9, it has been possible to drive E_F down in

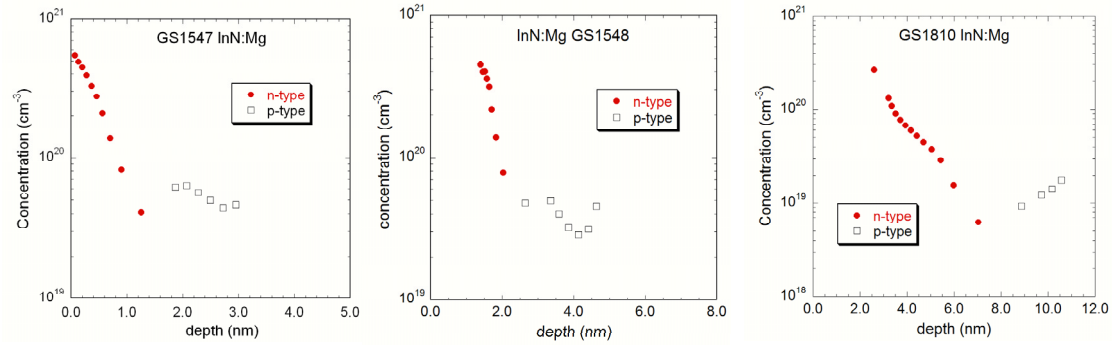

Fig. 10. ECV measurements ECV data demonstrating p-type doping in 3 InN:Mg films grown by MBE at Cornell. The surface Fermi level is pinned ca. 0.8 eV above the conduction band edge, leading to strong n-type character there. However, the bulk appears to be p-type.

p-GaN to a level that, if achievable in InN or in InGaN, would produce p-type material. We performed ECV measurements to investigate whether p-type activity could be observed below the surface electron accumulation layer in Mg-doped InN. As shown in Fig. 10, in all Mg-doped InN films studied, evidence of a type change from n to p-type below the surface was observed. However the existence of the p-type doping cannot be verified by measurements of the Hall effect as the conductivity is determined by the n-type surface inversion layer.

4.5 Task 5: Predict radiation service limits

This work has shown that the radiation resistance of In-rich InGaN is significantly higher than materials currently used in MJ cells. The minority carrier properties in n-type $In_{1-x}Ga_xN$ are stable to displacement damage doses (D_d) in the mid 10^{14} MeV/g range. Dose in the mid 10^{14} MeV/g range are required to seriously degrade the performance of the material. It is predicted that InGaN-based opto-electronics could operate in missions that would expose them radiation doses at least two orders of magnitude greater than those that render standard MJ cells inoperable.

5 Technological Outlook

The outstanding technological challenge in developing In-rich InGaN as an optoelectronic material is achieving p-type activity. When this is accomplished, the radiation testing done in this project can be repeated on pn junctions used for power conversion and the radiation hardness of an InGaN-based cell can be evaluated directly. Given what we have discovered about the surface accumulation layer and the position of the Fermi stabilization energy (E_{FS}) with respect to the conduction band edge, we believe a promising approach is to attempt to make pn junction in $In_{1-x}Ga_xN$ in the range of 0.3 – 0.6. At these compositions, E_{FS} is closer to the conduction band edge (it is resonant with it at x – 0.6) and p-type activity should be easier to achieve. In this context, the development of $In_{0.6}Ga_{0.4}N$ as a radiation resistant top cell with a gap of 1.9 eV appears promising. We note that the relatively low growth temperature required for InGaN and the insensitivity of the material to structural defects may enable integration with current MJ cell technology.

For research purposes, it is also possible to form pn junctions in other ways. p-$CuInS_2$ has suitable band offset to make a heterojunction; LBNL has made $CuInS_2$ films with correct band gap and p-type activity and is working on depositing them on n-InN. We are also exploring the low-temperature deposition of insulators on InN, with the goal of fabricating simple majority carrier devices. There is a recent report [Cimalla *et al.*, 2004] that sputtering of the InN surface can remove the surface accumulation layer. This, and related passivation techniques are expected to be applied to p-doped InN with the goal of making contact to the p-type material we have shown is below the surface.

In conclusion, we note the increasing level of world-wide interest in InN and In-rich InGaN that has arisen in the last two years. We are aware of more than 10 academic or government labs and at least one company (Blue Photonics Inc.) that can now produce high quality high-quality InN or InGaN epilayers using both MBE and MOCVD techniques. Many more laboratories are engaged in exploring the fundamental and technological and properties of this alloy system. Some evidence of this activity can be found in the proceedings of the First International Indium Nitride Workshop, which was organized by the Office of Naval Research and held in Freemantle, Australia [*J. Crystal Growth* **269**(1) 1-180 (2004)]. The topics for the second workshop in this series, which is being organized by the Air Force Office of Scientific Research and will be held in Hawaii in 1/05, will include discussion of device applications including, in addition to radiation resistant solar cells, millimeter wave FETs, bipolar transistors, high power light emitters, thermovoltaic cells, electro-chemical sensors, and Hz surface emitter. The work performed in this project supports the following statement made by the organizers of the Hawaii workshop:

> *InN semiconductor-based devices may play a strategic role in future DoD and commercial systems. Of particular interest are optoelectronic, high power millimeter wave and high speed switching devices.*

6 References

Bertness, K. A., S. R. Kurtz, D. J. Friedman, A. E. Kibbler, C. Kramer, and J. M. Olson, "29.5%-efficient GaInP/GaAs tandem solar cells," *Appl. Phys. Lett.* **65** 989-991 (1994).

Cimalla, V., G. Ecke, M. Niebelschütz, O. Ambacher, R. Goldhahn, H. Lu, and W. J. Schaff, "Surface conductivity of epitaxial InN," *Phys. Stat. Sol. C,* in press.

Doppalapudi, D., S. N. Basu, K. F. Ludwig Jr., and T. D. Moustakas, "Phase separation and ordering in InGaN alloys grown by molecular beam epitaxy," *J. Appl. Phys.* **84** 1389-1395 (1998) and references therein.

El-Masry, N. A., E. L. Piner, S. X. Liu, and S. M. Bedair, "Phase separation in InGaN grown by metalorganic chemical vapor deposition," *Appl. Phys. Lett*. **72**, 40-3 (1998).

Flood, D. J., "Advanced Space Solar Cells," *Prog. Photovolt: Res. Appl.* **6**, 187-192 (1998).

Green, M. A., K. Emery, D. L. King, S. Igari, and W. Warta, "Solar Cell Efficiency Tables (Version 21)," *Prog. Photovolt: Res. Appl*. **11**, 39-45 (2003) and references therein.

Ho, I.-h., and G. B. Stringfellow, "Solid phase immiscibility in GaInN," *Appl. Phys. Lett*. **69**, 2701-2703 (1996).

Kim, K. S., A. Saxler, P. Kung, M. Razeghi, Y. Lim, "Determination of the band-gap energy of $Al_{1-x}In_xN$ grown by metal–organic chemical-vapor deposition," *Appl. Phys. Lett.* **71** 800-803 (1997).

Li, S. X., J. Wu, E. E. Haller, W. Walukiewicz, W. Shan, H. Lu, and W. J. Schaff, "Hydrostatic pressure dependence of the fundamental bandgap of InN and In-rich group III nitride alloys," *Appl. Phys. Lett.* **83**, 4963-4965 (2003).

Lu, H., William J. Schaff, Jeonghyun Hwang, Hong Wu, Wesley Yeo, Amit Pharkya, and Lester F. Eastman, "Improvement on epitaxial grown of InN by migration enhanced epitaxy," *Appl. Phys. Lett.* **77** 2548-2550 (2000).

Lu, H., Schaff, W.J.; Jeonghyun Hwang; Hong Wu; Koley, G.; Eastman, L.F. Source "Effect of an AlN buffer layer on the epitaxial growth of InN by molecular-beam epitaxy," *Appl. Phys. Lett.* **79** 1489-91 (2001).

Mahboob, I., T. D. Veal, C. F. McConville, H. Lu and W. J. Schaff, "Intrinsic Electron Accumulation at Clean InN Surfaces," *Phys. Rev. Lett.* **92**, 036804 (2004)

Messenger, S. R., E. A. Burke, G. P. Summers, M. A. Xapsos, R. J. Walters, E. M. Jackson, and B. D. Weaver, "Nonionizing Energy Loss (NIEL) for Heavy Ions," *IEEE Trans. Nuclear Sci.* **46**, 1595-1602 (1999).

Messenger, S. R., G. P. Summers, E. A. Burke, R. J. Walters, and M. A. Xapsos, "Modeling Solar Cell Degradation in Space: A Comparison of the NRL Displacement Damage Dose and JPL Equivalent Fluence Approaches," *Prog. Photovolt: Res. Appl.* **9**, 103-121 (2000).

Nolte, D. D., "Surface recombination, free-carrier saturation, and dangling bonds in InP and GaAs," *Solid State Electronics* **33**, 295-8 (1990).

Pereira, S., M.R. Correia, T. Monteiro, E. Pereira, E. Alves, A.D. Sequeira, N. Franco, "Compositional dependence of the strain-free optical band gap in $In_xGa_{1-x}N$ layers," *Appl. Phys. Lett.* **78,** 2137-9 (2001).

Rao, M., D. Kim, and S. Mahajan, "Compositional dependence of phase separation in InGaN layers," *Appl. Phys. Lett.* **75,** 1961-1963 (2004).

Shan, W., J.W. Ager III, K.M. Yu, W. Walukiewicz, E.E. Haller, M.C. Martin, W.R. McKinney, W. Yang, "Dependence of the fundamental band gap of $Al_xGa_{1-x}N$ on alloy composition and pressure," *J. Appl. Phys.* **85** 8505-8507 (1999).

Sumita, T., M. Imaizumi, S. Matsuda, T. Oshima, A. Ohi, and H. Itoh, "Proton radiation analysis of multi-junction space solar cells," *Nuc. Instrum. Methods Phys. Res.* B **206** 448-451 (2003).

Vurgaftman, I. and J. R. Meyer, "Band parameters for nitrogen-containing semiconductors," *J. Appl. Phys.* **94**, 3675-3696 (2003) and references therein.

Wakahara, A., T. Tokuda, X.-Z. Dang, S. Noda, and A. Sasaki, "Compositional inhomogeneity and immiscibility of a GaInN ternary alloy," *Appl. Phys. Lett*. **71**, 906-9 (1997).

Walukiewicz, W., "Amphoteric native defects in semiconductors," *Appl. Phys. Lett*. **54**, 2094-6 (1989).

Walukiewicz, W., "Intrinsic limitations to the doping of wide-gap semiconductors," *Physica* B, **302**, 123 (2001).

Wu, J., W. Walukiewicz, K.M. Yu, J.W. Ager III, E.E. Haller, H. Lu, W.J. Schaff, Y. Saito, Y. Nanishi, "Unusual properties of the fundamental band gap of InN," *Appl. Phys. Lett.* **80** 3967-3769 (2002a).

Wu, J., W. Walukiewicz, K.M. Yu, J.W. Ager III, E.E. Haller, H. Lu, W.J. Schaff, "Small band gap bowing in $In_{1-x}Ga_x/N$ alloys," *Appl. Phys. Lett.* **80** 4741-4743 (2002b).

Wu, J., W. Walukiewicz, K. M. Yu, W. Shan, J. W. Ager III, E. E. Haller, H. Lu, and W. J. Schaff, W. K. Metzger, S. R. Kurtz, J. F. Geisz, "Superior radiation resistance of $In_{1-x}Ga_xN$ alloys: a full-solar-spectrum photovoltaic material system, *J. Appl. Phys.* **94**, 6477-6482 (2003a).

Wu, J., W. Walukiewicz, K.M. Yu, J.W. Ager, S.X. Li, E.E. Haller, H. Lu, and W.J. Schaff, "Universal bandgap bowing in group-III nitride alloys," *Solid State Commun.* **127**, 411 (2003b).

Yamaguchi, M., "III-V compound multi-junction solar cells: present and future," *Solar Energy Mat. and Solar Cells* **75**, 261-9 (2003) and references therein.